Chemical Engineering Solution for Carbon Neutrality in Cement Industrial: Tailor the Pathway from Inevitable CO_2 Emission into Syngas

Bin Shao[1,2,†], Yuanming Zhu[2,†], Jun Hu[*1], Yuan Zong[3], Zhicheng Xie[1], Su Li[1], Wenli Du[2], Meihong Wang[*4], Honglai Liu[1,3], Feng Qian[*2]

Affiliations

[1] School of Chemistry and Molecular Engineering, East China University of Science and Technology, 130 Meilong Road, Shanghai 200237, China.

[2] Key Laboratory of Smart Manufacturing in Energy Chemical Process, Ministry of Education, School of Information Science and Engineering, East China University of Science and Technology, 130 Meilong Road, Shanghai 200237, China.

[3] State Key Laboratory of Chemical Engineering, School of Chemical Engineering, East China University of Science and Technology, 130 Meilong Road, Shanghai 200237, China.

[4] Department of Chemical and Biological Engineering, The University of Sheffield, Sheffield S1 3JD, United Kingdom.

[†] These authors contributed equally: Bin Shao, Yuanming Zhu

Contributions

J. H., M. W. and F. Q. supervised the research. J. H. and B. S. conceived the ideas and designed the present work. B. S. and S. L. synthesized the catalysts and carried out all of the performance experiments.

B. S., Z. X. and Y. Z. performed the process simulations and conducted the analysis. H. L. and Y. Z. provided constructive suggestions. B. S. wrote the manuscript. J. H., M. W. and F. Q. contributed to manuscript editing. All authors discussed the results and assisted during manuscript preparation.

Corresponding authors

Correspondence to: Jun Hu, Meihong Wang and Feng Qian

*E-mails: junhu@ecust.edu.cn, meihong.wang@sheffield.ac.uk, fqian@ecust.edu.cn

Abstract

Cement production is one of the largest industrial sources of CO_2 emissions due to the thermal decomposition of limestone ($CaCO_3$). We combine the chemical engineering strategy into the cement production and propose a novel process of "Carbonate Dry Reforming of Methane (CaDRM)" that converts the limestone ($CaCO_3$) directly into the cement clinker precursor (CaO) and syngas ($CO+H_2$) through reacting with methane (CH_4). Thermodynamic analysis indicates the reaction temperature of CaDRM is lowered by at least 200°C compared with $CaCO_3$ thermal decomposition. Lab scale experimental studies show a 95% CaO yield at a 91% syngas selectivity and 90% CH_4 conversion in CaDRM using cement raw meal at 700°C. Process simulation scale-up and economic analysis indicate CaDRM pathway can reduce 37.2% CO_2 emission in comparison with the conventional $CaCO_3$ thermal decomposition pathway. More significantly, the net profit of $271.0/t (clinker) can be achieved by the value-added syngas products and the energy saving. The economic and environmental benefits of the proposed CaDRM strategy can help its future commercial deployment.

Introduction

Thermal decomposition of inorganic metal carbonates is one of the most important chemical processes in industries including cement, steel and non-ferrous metals metallurgy[1-3]. Nevertheless, the high-temperature decomposition of carbonates is inevitably accompanied by massive CO_2 emissions and huge energy consumptions. Among them, the cement production (2.8 Gt/y) is currently the largest single industrial source of carbon emissions, accounting for about 8% of global CO_2 emissions[4]. Analysis along the carbon footprint of the cement production reveals process-related CO_2 emissions from the decomposition of limestone ($CaCO_3$) (**Eq. 1**) in the pre-calciner account for more than 60% of total emissions and energy-related CO_2 emissions from the combustion of fossil fuel for maintaining high temperatures of rotary kiln (1,450°C-1,500°C) and pre-calciner (~900°C) account for the left 40% of total emissions (**Figure 1a, black pathway**) [5].

To reduce the carbon emissions from the cement industry, many chemical engineering strategies have been proposed in the cement production, including using the carbonate-free raw materials[6-8], replacing the energy supplies with renewable energies[9,10] and implementing carbon capture, utilization and storage (CCUS) technologies[11,12]. Specifically, when the captured CO_2 is used as a feedstock to produce valuable fuels and chemicals through various hydrogeneration processes such as Fischer-Tropsch and methanation[13-16], it might compensate for some capital investments and operation costs of CO_2 capture. However, facing the challenges of the huge production but relatively low profits[17,18], the cement industry is keenly aware of difficulties to bear high-cost carbonate-free raw materials, renewable energies, and additional high costs of CCUS technology[19,20]. Therefore, it is of great urgency to develop innovative

technologies to achieve the carbon neutrality in cement industry.

$$CaCO_3(s) \rightleftharpoons CaO(s) + CO_2(g) \quad (1)$$

$$CaCO_3 + CH_4 \rightarrow CaO + 2CO + 2H_2 \quad (2)$$

$$CaCO_3(s) + H_2(g) \rightarrow CaO(s) + CO(g) + H_2O \quad (3)$$

We propose a novel strategy of direct reduction of carbonate by methane, namely Carbonates Dry Reforming of Methane (CaDRM) (**Figure 1a, orange pathway**). Different from conventional dry reforming of methane (DRM) with captured CO_2 from the process-related and energy-related emissions [21,22], the proposed CaDRM strategy lies in the methane reforming of the carbonate in one chemical process without producing any CO_2 but syngas (H_2+CO) production (**Eq. 2**). One inherent benefit of such a process is that it allows the simultaneous productions of clinker- precursor (CaO) and valuable syngas. In addition, the overall energy penalties are expected to be significantly reduced due to the integrated processes, avoiding the temperature swing between CO_2 capture and utilization, as well as consequent treatments after the CO_2 capture such as desorption, compression, and transportation. So far, to the best of our knowledge, there is no report on the direct reduction of carbonates by CH_4. Fortunately, an interesting observation reported by Giardini et al. [23] and Reller et al. [24] on the possibility of the degradation of carbonates in a H_2 atmosphere to form hydrocarbon at comparably low temperatures (**Eq. 3**). Baldauf-Sommerbauer et al.[25] illustrated the feasibility of reduction of iron ores ($FeCO_3$) with hydrogen, which can theoretically decrease CO_2 emissions by 60% and reduce agent up to 33% for iron production. Very recently, Wu's group[26] and Duan's group [27,28] both found the auto-catalytic activity of the hydrogenation reduction of calcium carbonates for the migration of CO_2 emission into CO and CH_4

productions. Compared with those carbonate hydrogenation, the proposed CaDRM strategy can be a more efficient way to change CO_2 emissions into syngas production due to the fully atomic utilization efficiency of CH_4[29-31]. More significantly, in comparing with H_2 source, CH_4 possesses more advantages such as the abundancy in nature (nature gas), mature industrial applications, and most importantly being cost-effective[32,33]. Inspired by our previous study of integrated CO_2 capture and conversion which explicitly identified the synergistic promotion of the carbonate reduction by CH_4 for the regeneration[34] , we highly anticipate the CaDRM strategy can bring a disruptive technological revolution for achieving net-zero in the CO_2 emission-intensive cement industry.

Herein, combining the thermodynamic analysis and experimental verifications, we firstly demonstrated the feasibility of CaDRM that the reaction temperature can be lowered by at least 200℃ in comparison with the thermal $CaCO_3$ decomposition. Furthermore, with the help of Ni/CaO catalyst, not only the $CaCO_3$ powder, but also the real cement raw meal can successfully achieve a 95% CaO yield with at a least 91% syngas selectivity and 90% CH_4 conversion at lower temperature of 700℃. In addition, to distinguish the carbon mitigation advantages of the CaDRM process, a comparative process of $CaCO_3$ thermal decomposition with the CO_2 capture and utilization (CCU) processes of MEA-scrubbing and DRM was established as well. Economic assessment based on the process simulations further illustrated the significance of CaDRM by the comparisons of the energy consumption, CO_2 emissions, and operating costs. As such, the proposed CaDRM process can be a promising strategy to synergistically reduce the carbon emissions from both sides of the production pathway and energy conservation.

Results and discussion

Thermodynamic analysis

To evaluate the feasibility of the proposed CaDRM strategy, thermodynamic analysis was firstly performed by comparing the reductive decomposition of $CaCO_3$ in a CH_4 atmosphere with the conventional $CaCO_3$ thermal decomposition. CaDRM reaction depends much on the temperature and becomes thermodynamic favorable since its Gibbs free energy is lower than the $CaCO_3$ thermal decomposition above 630℃ (**Figure 1b**). More importantly, the CaDRM reaction starts at as low as 475℃, and completes at 700℃ (**Figure 1c**), which is about 200℃ lower than the theoretical complete convention of the $CaCO_3$ thermal decomposition at 900℃. Whereas at 700℃, the conversion of $CaCO_3$ thermal decomposition is only 5.4%. Therefore, the direct reduction of $CaCO_3$ by methane in CaDRM is thermodynamically feasible, not only lowering down the total energy penalty of $CaCO_3$ thermal decomposition through reducing decarboxylation temperature, but also removing CO_2 emissions from the production source[35].

In addition to the direct reduction of $CaCO_3$ by CH_4, CaDRM is actually a complex system with multiple side reactions occurring simultaneously, such as the thermal decomposition of $CaCO_3$, CH_4 cracking, CO_2 hydrogenation, reversible water-gas-shift reaction (RWGS) (**Eq. S1-S5, SI**). To predict the operating temperature windows, we calculated the composition distributions of all possible products along with the temperature in the complex CaDRM system (**Figure S1**). Below 650°C, the $CaCO_3$ decomposition is unfavorable, whereas the CH_4 cracking is thermodynamically dominant, giving a significantly increased H_2 generation and carbon deposit[36]. When raising the temperature to above 700℃,

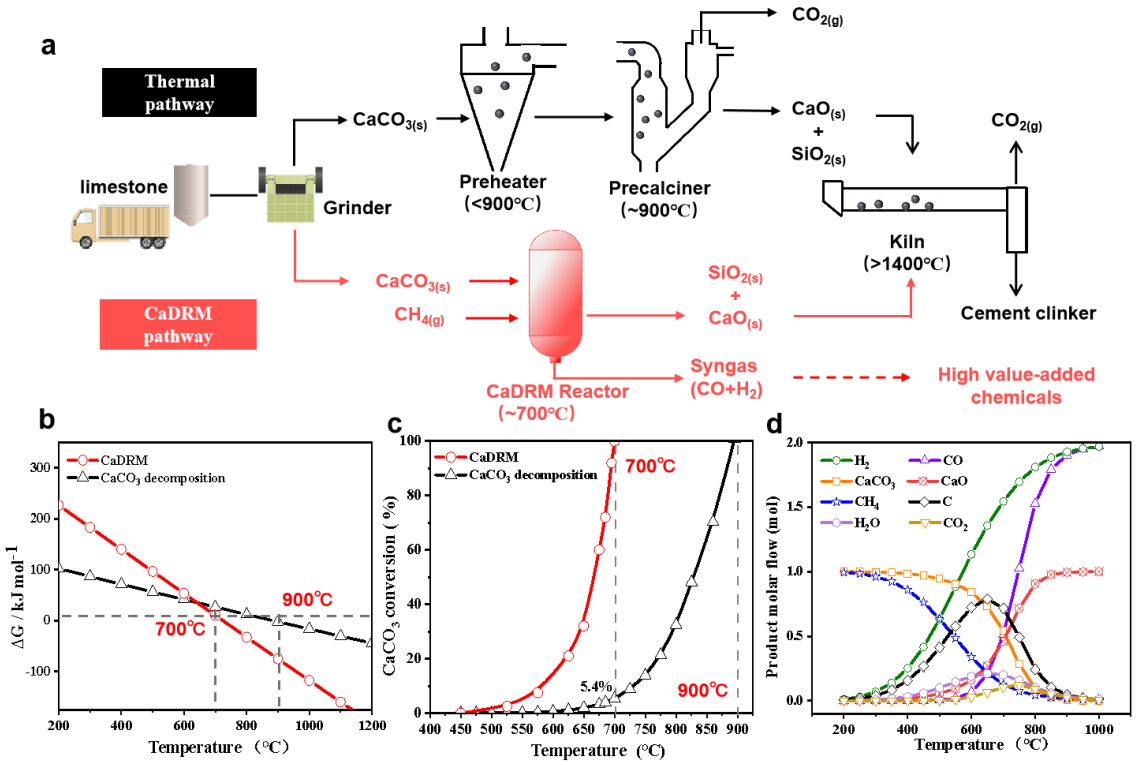

Figure 1 Comparison of CaDRM pathway with conventional $CaCO_3$ thermal decomposition for cement clinker production. (a) overview of the incumbent thermal decomposition process (black) and the proposed CaDRM process (orange) for manufacturing cement clinker. In the thermal pathway, limestone ($CaCO_{3(s)}$) is heated to above 900 ºC in the precalciner for the $CaCO_{3(s)}$ decarbonate into $CaO_{(g)}$ and $CO_{2(g)}$. In the CaDRM pathway, $CaCO_3$(s) is converted with $CH_{4(g)}$ into $CaO_{(s)}$ in a CaDRM reactor which also generates valuable syngas ($CO_{(g)}$ and $H_{2(g)}$). (b) Gibbs free energy of $CaCO_3$ thermal decomposition and CaDRM reactions as a function of temperature. (c) The relationship between the decomposition conversion rate of $CaCO_3$ and temperature. (d) The effect of reaction temperature on the distributions of most probable products in CaDRM system with considering the slide reactions at 1 atm and CH_4 to carbonate molar ratios of 1:1.

the transition decline of carbon deposit and rapid increase of CO suggest the CaDRM reaction is dominant. When the temperature further increases to above 850°C, the complete decomposition of $CaCO_3$is achieved and the formation rate of H_2, CO and CaO reaches the maximum values, respectively. Notably, during the whole temperature region, the content of CO_2 composition is very low. After an initial

small increase, it decreases again and completely eliminates when the temperature is up to 800ºC. Therefore, the system of CaDRM is primarily temperature-dependent and high temperature is beneficial for the CO_2 DRM, RWGS, and CaDRM (**Figure 1d)**. Furthermore, increasing the initial molar ratio of CH_4 to $CaCO_3$, the H/C molar ratio in the syngas production can be effectively controlled, but the carbon deposit inevitably occurs due to the excessive CH_4 cracking (**Figure S1**). This needs to be addressed to maintain the quality of clinker production.

Experimental verifications

To experimentally verify the proposed CaDRM route, we investigated the CaDRM performance in a fixed-bed column with an inner diameter of 10 mm in the temperature range of 700 - 800℃ (**Figure S2**). A cement compatible catalyst of Ni/CaO was applied to drive the proposed CaDRM process. Prepared by a simple one-pot sol-gel method, the X-ray diffraction (XRD) pattern (**Figure 2a**) of as-synthesized Ni/CaO evidence the presence of NiO with its (200) diffraction peak at 2θ=43.2˚. The average crystallite size was calculated to be 25.6 nm based on the Scherrer equation. The scanning electron microscope (SEM) image shows Ni/CaO catalyst is composed of the aggregated nanoparticles (**Figure 2b**), with a Brunauer–Emmett–Teller specific area of 21.0 m^2 g^{-1} and a mean pore size of 50 nm (**Figure S3**). The HAADF-STEM and the energy-dispersive X-ray elemental mapping images reveal that NiO particles are highly dispersed in the CaO matrix. High-resolution transmission electron microscope (HRTEM) image further illustrates the high crystallinity of the hexagonal NiO, with clear (200) lattice fringes of 0.208 nm spacing (**Figure 2c-2f)**.

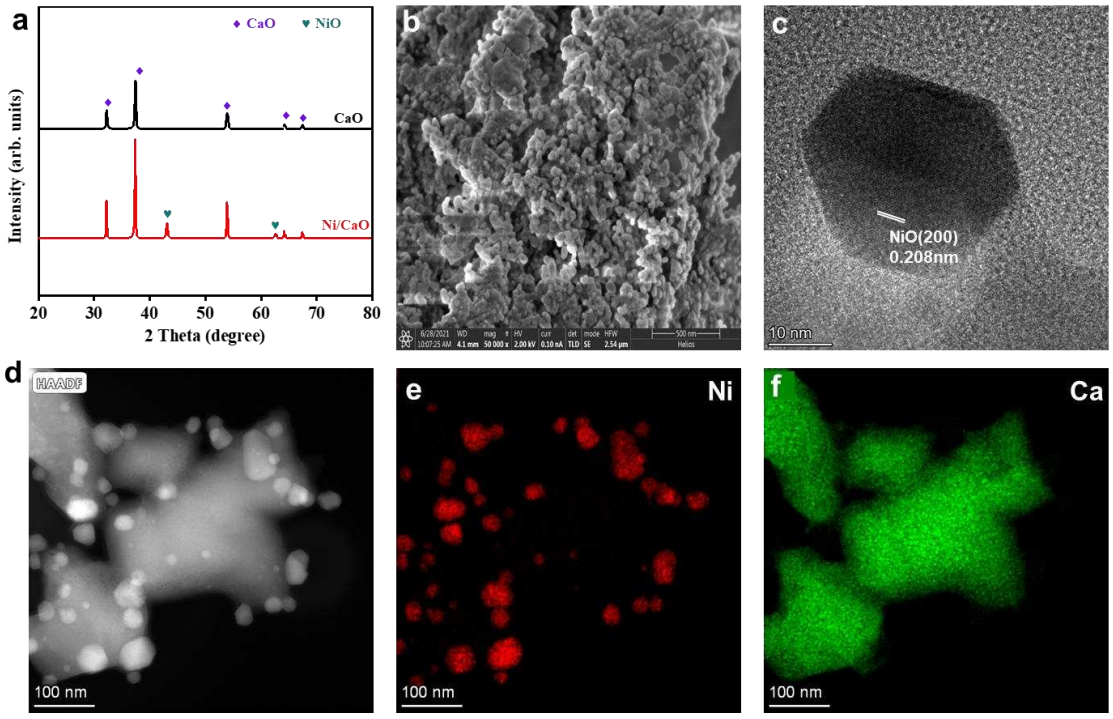

Figure 2 Structural characterization of catalyst. (a) XRD pattern of CaO and Ni/CaO. (b) SEM image of Ni/CaO. Scale bar, 500 nm. (c) HRTEM of Ni/CaO. Scale bar, 10 nm. (d) STEM image of Ni/CaO. (e-f) Energy-dispersive X-ray elemental mapping of Ni/CaO. Scale bar, 100 nm.

As expected, with the help of Ni/CaO catalyst, the degradation of $CaCO_3$ starts at lower temperature of 700 °C in a CH_4 atmosphere, the decarbonation shows a sharp triggering and complete in 45 min (**Figure 3a and 3b**). After the magnetic separation of the Ni/CaO catalyst (**Figure S4**), the XRD pattern of the solid products of catalytic CaDRM shows the characteristic peaks of CaO, containing very week peaks of $Ca(OH)_2$ due to the atmospheric humidity (**Figure 3c**). The calculated conversion efficiency of $CaCO_3$ is as high as 95% (**Figures 3d and S5**). Meanwhile, the generation of CO and H_2 (syngas) can be clearly observed after the triggering in the gaseous elution, with the molar ratio of H_2: CO: CO_2 of 17.2:14.3:1. The produced syngas shows a high selectivity of 96.9% and the reaction rate could be up to 0.38 mmol min^{-1}, which can be further applied to the Fischer-Tropsch reactions for producing high value-

added chemicals and fuels. In contrast, without adding any catalysts, a very slow decarbonation occurs as the conventional $CaCO_3$ thermal decomposition due to the formidable activation energy necessary to disrupt the stable C–H bond within the methane molecule. It takes more than 90 min to accomplish the surface decomposition at 700℃. The XRD pattern further indicates the existing of CaO in solid products, but a large amount of $CaCO_3$ remained (**Figure S6**), and the conversion efficiency of $CaCO_3$ is as low as 50.3% (**Figure 3d**). No CO signal can be observed in the whole detecting temperature range in the gaseous elution curve, except for a CO_2 peak starting at 780℃ and H_2 at up to 800℃ (**Figure S7**). These inconsistent experimental results indicate that although CaDRM reaction is thermochemically favorable, the actual process could be kinetically limited without proper catalysts.

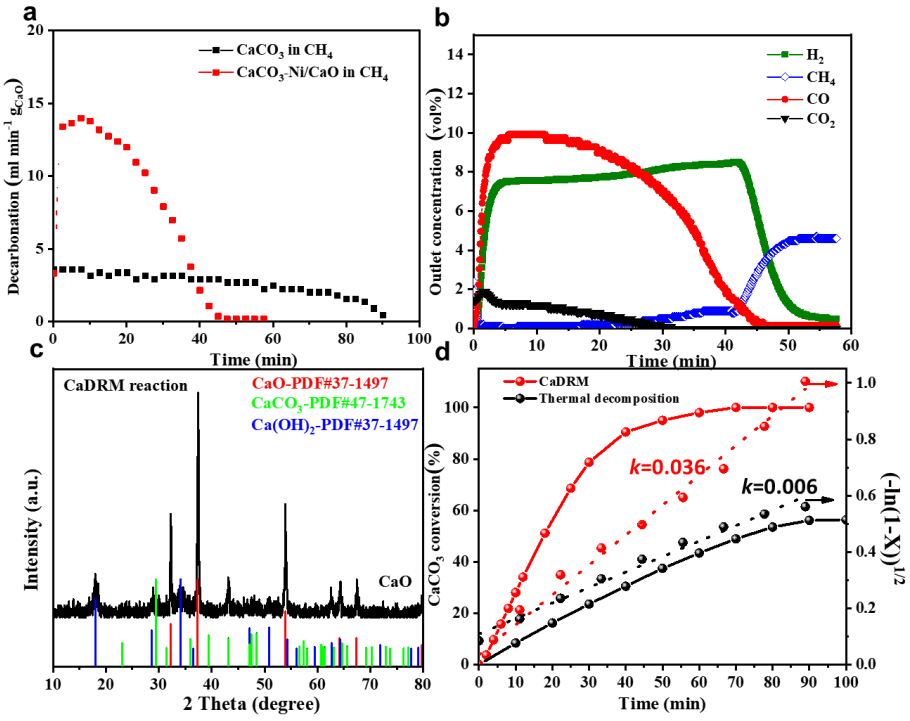

Figure 3 Comparison of decarbonation kinetics between the CaDRM and the conventional $CaCO_3$ thermal decomposition. (a) Decarbonation rate as a function of time at 700℃. (b) Molar flow rates of CO, H_2 CH_4 and CO_2 in the gaseous elution of CaDRM reaction. (c) The XRD patterns of solid products of CaO and $Ca(OH)_2$ obtained from CaDRM at 700℃. (d) The conversion rates of $CaCO_3$ and its

dynamic fitting curves of CaDRM and $CaCO_3$ thermal decomposition under 700℃.

Notably, the shortened reaction time required to accomplish CaDRM is almost a half of that required for conventional $CaCO_3$ thermal decomposition at 700℃. The kinetic analysis of the gas-solid heterogeneous decarbonation of $CaCO_3$ in different pathways of CaDRM and thermal decomposition were further illustrated. Fitted well by the modified Avrami-Erofeev (A-V) Equation, respectively ($R^2 >$ 0.9889), the value of the kinetic constant (k) of CaDRM route is calculated as high as 0.036, 6-time higher than the k of 0.006 of $CaCO_3$ thermal decomposition at 700℃ (**Figure 3d**). This can be attributed to the effect of Le Chatelier's principle, that the continuous consumption of the CO_2 from $CaCO_3$ by the CH_4 reforming on the catalytic sites of Ni can significantly shift the thermodynamic equilibrium of the $CaCO_3$ decomposition, providing an additional driving force for fast decarbonation[37].

Inspired by the excellent performance of high conversion efficiencies and superior reaction kinetics of $CaCO_3$ at the lower temperature, we validated the CaDRM using real cement raw meals. The average particle size of raw meal is in the range 50-100 um, and the compositions are very complex, consisting of 71.43% $CaCO_3$ and other remains such as Si, Fe, Al by ICP-OES. Excitingly, the molar flow rate of CH_4, CO, H_2 and CO_2 in the gaseous elution demonstrate the success of the CaDRM in reality, that a complete $CaCO_3$ conversion at a 100% CO selectivity with 90% methane utilization efficiency can be perfectly achieved at 700℃ **(Figure 4a and 4b)**. During the CaDRM process, the $CaCO_3$ concentration decreases with time, accordingly, the whole process can be divided into three stages. The first very fast stage (0-10 min), the sharply increased flows of H_2 and CO with only a little unconverted CO_2 and CH_4 in the elution indicate an almost complete conversion of CH_4 with $CaCO_3$ into syngas. The molar ratio of H_2 to CO is about 0.9, lower than the predicted thermodynamic equilibrium for the CaDRM at 700℃, suggesting that

produced H_2 may also participate in the $CaCO_3$ hydrogenation[38]. In the second stable stage (10-35 min), the decline of CO_2 flow can be ascribed to the depletion of $CaCO_3$. While the gradually decreased CO flow but the stable H_2 one suggests the water-gas-shift reaction by consuming CO to produce H_2 may occur[39]. In the last stage (>35 min), the gradually increased CH_4 flow and the decreased CO flow demonstrate the almost complete $CaCO_3$ conversion. Meanwhile, the simultaneously decreased H_2 flow indicates that the CH_4 cracking seldom occurs at 700℃.

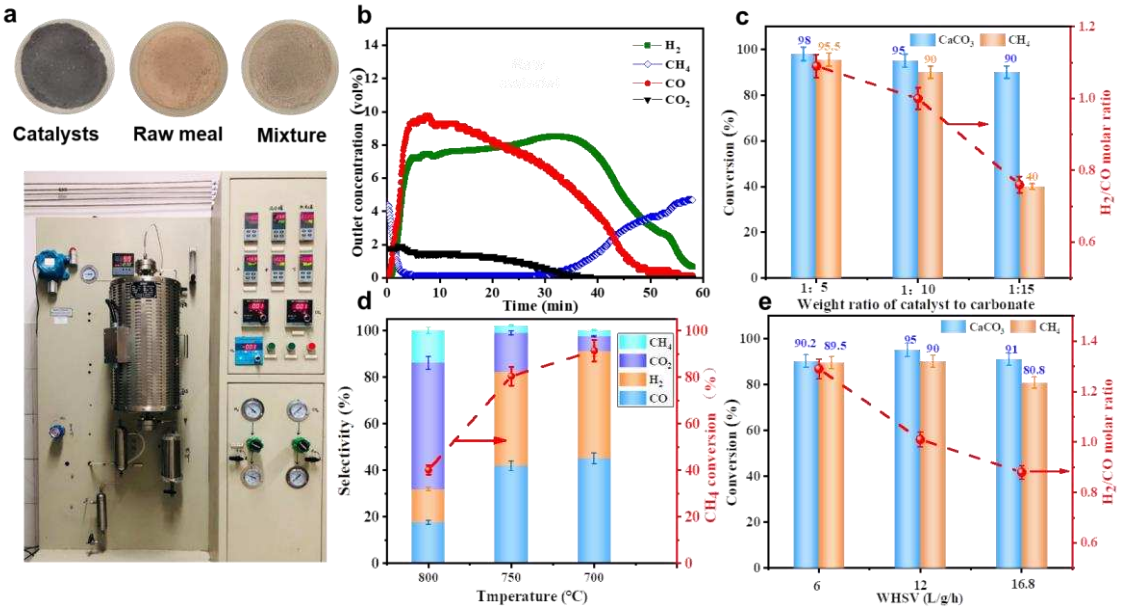

Figure 4 The CaDRM performance of real cement raw meals over Ni/CaO catalyst. (a) The fixed-bed device with the mixture of catalysts and cement raw meal for CaDRM process. (b) Molar flow rates of CO, H_2 CH_4 and CO_2 in the gaseous elution during CaDRM reaction. (c) The effect of catalyst ratio on calcium carbonate and CH_4 conversion rate. (d) The selectivity of product gas of CaDRM reaction at different temperature. (e) Calcium carbonate and CH_4 conversion rate a at different weight hourly space velocity (WHSV) of methane. The error bars represent the standard deviation of three independent measurements.

Furthermore, we optimized the operating conditions to enhance the CaDRM performance. By optimizing the weight ratio of catalyst to cement raw meal at 1:10, the $CaCO_3$ and CH_4 conversion

efficiency of 95% and 90%, with syngas selectivity of 91.0%, can be achieved, respectively (**Figures 4c and S8a**). In addition, consistent with the thermodynamic predictions, the reaction temperature plays a pivotal role in selectivity of syngas and conversion of $CaCO_3$. The complete conversion time of cement raw meals shortens with rising reaction temperature, from 45 min at 700℃ to 15 min at 800℃, but the selectivity of syngas including CO and H_2 decreases significantly from 91.0% to 31.8% (**Figures 4d** and **S9**), which can be caused by the competitive thermal decomposition of $CaCO_3$. Moreover, the weight hourly space velocity (WHSV) of the CH_4 feed were also investigated. Along with increasing WHSV from 6 L g^{-1} h^{-1} to 16.8 L g^{-1} h^{-1}, methane and carbonate conversion rate increases first to a maximum and then decreases, however, the selectivity of syngas decreases from 93.9% to 82.2% which can be attributed to the lower methane conversion (**Figures 4e and S8b)**. Moreover, the higher WHSV means the shortened residence time of gas-solid reaction, so the methane conversion and the molar ratio of H_2/CO decrease at higher WHSV. Therefore, a suitable WHSV of CH_4 is 12 L g^{-1} h^{-1} for a high selectivity of syngas and regulating the H_2/CO ratio of 1.0 (**Table S1**). Notably, the XRD patterns of the cement raw meal and the obtained solid products of dominated CaO further confirm the validity of CaDRM (**Figure S10**), which can subsequently produce the clinker precursor in the kiln. As such, CaDRM will be a promising strategy for future large scale cement production with low carbon emission and low energy consumption.

Process Simulation and Preliminary Economic Evaluation

To demonstrate the practical feasibility of CaDRM at large scale, we carried out the process simulation. As CaDRM is the integration of both remarkably endothermic $CaCO_3$ thermal decomposition

and the DRM reaction, it requires close attention to the heat supply. In this context, we integrated the process of oxygen enriched combustion of CH_4 with the CaDRM process, namely auto-thermal CaDRM, since CH_4 acts as both reactant and fuel for the energy supply. By using the Aspen Plus V10®, the model of the clinker production system based on the auto-thermal CaDRM route was constructed, which was composed of the air separator unit (ASU), heat exchange cyclones, CH_4 combustion furnace, CaDRM reactor, rotary kiln and pressure swing adsorption unit (PSA) for purification of syngas, respectively (**Figure 5a**). For the sake of comparison, the referenced clinker production system based on the conventional $CaCO_3$ thermal decomposition route was also constructed by combining the additional CO_2 capture and utilization (CCU) unit. In comparison with CaDRM route, the CCU unit is composed of the monoethanolamine (MEA) scrubbing for CO_2 capture, which is currently employed in conventional cement industry and following the DRM reaction for the CO_2 utilization[40,41]. (**Figures 5b** and **S11**). To simulate the typical medium sized cement production line with the clinker production capacity of 2500 t/d (**Tables S2 and S3**), we set the decomposition rate of carbonate in cement raw meal as 95%, and the CH_4 conversion efficiency as 90%, respectively. The accuracy of the model was first verified by using the same compositions and feed rate of cement raw meal in the reported conventional clinker-production system based on the $CaCO_3$ thermal decomposition route (**Tables S4 and S5**)[42].

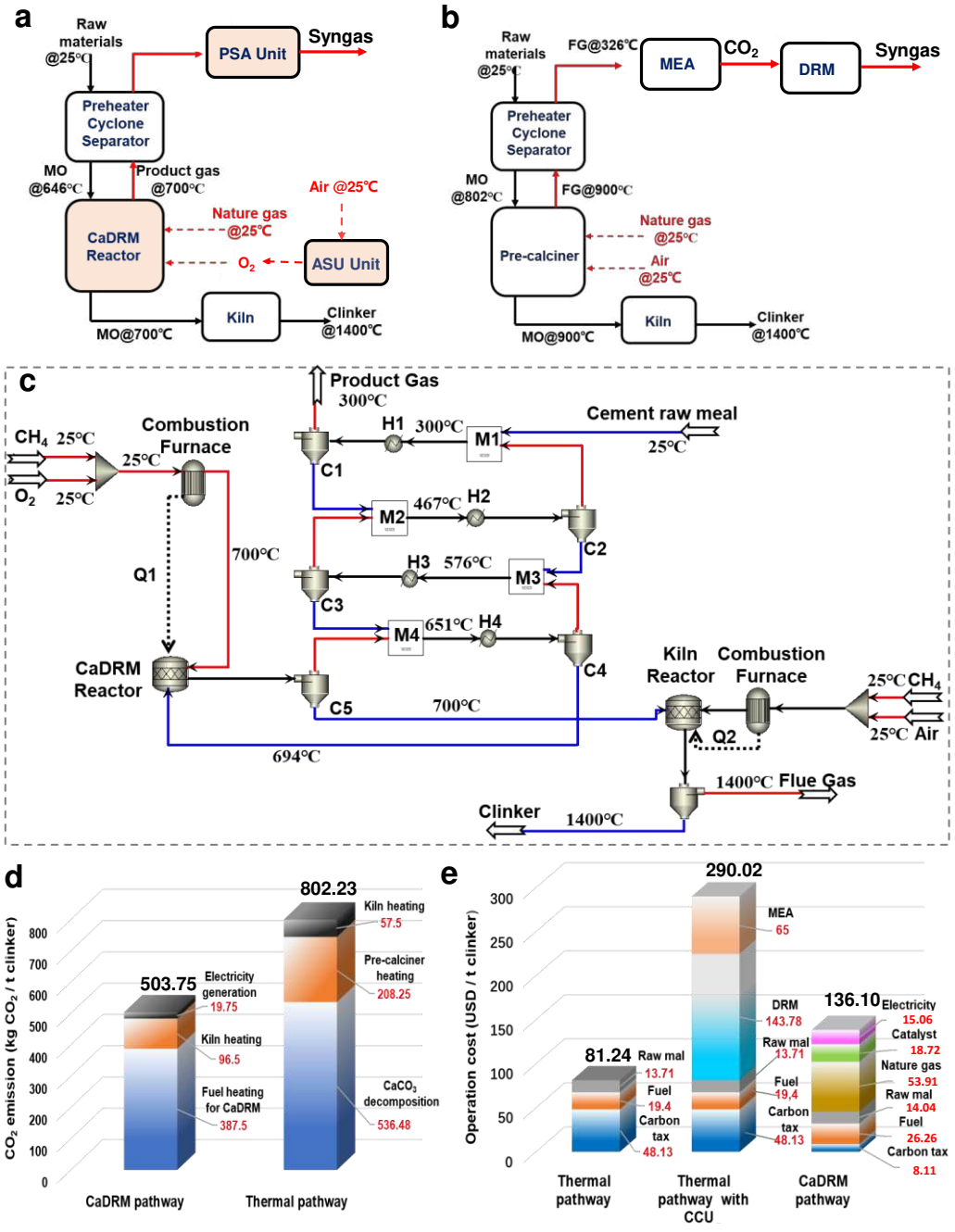

Figure 5. Process layouts and economic analysis of clinker and syngas co-productions through CaDRM route instead of the conventional $CaCO_3$ thermal decomposition. (a) the auto-thermal CaDRM system with ASU and PSA units. (b) the conventional $CaCO_3$ thermal decomposition system with CCU units. (c) Process model of the CaDRM system in Aspen Plus®. (d) CO_2 emissions analysis and comparison between two routes of the CaDRM and the conventional thermal decomposition. (e) Operating costs of the thermal decomposition pathway with/without CCU and CaDRM pathway.

The total energy consumption of the constructed clinker production systems includes three parts: 1) the heating supplies for the CaDRM reaction or $CaCO_3$ thermal decomposition; 2) the heating supplies for the high-temperature conversion of metal oxides to clinker in kilns; 3) the energy (electricity) supplies for ASU and PSA units in the CaDRM route, or for the CO_2 capture and conversion in the $CaCO_3$ thermal decomposition route. The CO_2 emissions of two systems were converted based on carbon intensity of electricity and the total fuels used for the energy supplies. We also estimated the operating costs based on the cost of the raw meal, CH_4 as the reactant and fuels, catalysts, electricity, and carbon tax of US $60 per ton CO_2 (Details can be found in SI). To simplify, we did not consider the heat recovery from the kiln and the heat loss of flue gas from the CaDRM reactor or the pre-calciner in both cases.

Table 1 Economic assessment of clinker and syngas productions through the CaDRM route.

Operating cost (thousand $ per day)		**Income (thousand $ per day)**	
Raw meal	35.10	Clinker	137.50
catalyst	46.80	Syngas	880.25
Electricity	37.64		
Nature gas	200.43		
CO_2 tax	20.29		
Total	340.26	Total	1017.75
Operating cost	$136.10/t (clinker)	Average income	$407.10/t (clinker)
Net income		$271.00/t (clinker)	

[a] Total CO_2 tax on heating for CaDRM reactor and calciner by burning natural gas.

On the premise of ensuring consistent feeds of the raw meal and output of clinker products, the balance of materials and energies of each system were calculated, respectively. (**Figures 5c** and **S12,**

Tables S6 and **S7**). Based on these, the economic analysis of two systems were evaluated by comparing the CO_2 emissions, energy supplies, and operating costs. The proposed system of CaDRM route can significantly reduce the inevitable carbon emissions of 536.48 kg (CO_2)/t (clinker) into the syngas by replacing the thermal decomposition of $CaCO_3$ with the reduction in a CH_4 atmosphere. Although the CaDRM process successfully decreases the operating temperature by 200°C, the strongly endothermic CaDRM reaction plus the consequent high temperature sintering in kilns (1450°C) need additional heat supplies, resulting in increases of CO_2 emissions by 218.25 kg (CO_2)/t (clinker). Moreover, to purify the syngas, the CO_2 emission related to electricity of ASU and PSA unit accounts for 19.75 kg(CO_2)/t (clinker). Thus, the CO_2 emissions of the CaDRM system can be significantly reduced by 37.2%, from 802.23 kg (CO_2)/t (clinker) of the conventional $CaCO_3$ thermal decomposition to 503.75 kg (CO_2)/t (clinker) in overall (**Figure 5d**). Meanwhile, the total energy supplies for the CaDRM system, including the units of ASU, oxy-combustion, CaDRM reactor, and PSA, are calculated as high as 6.54 GJ/t (clinker). Although this value is higher than the sole value of the conventional $CaCO_3$ thermal decomposition of 2.38 GJ/t (clinker), when considering the syngas production for the same evaluation level, the coupled CO_2 capture and conversion units of 10.46 GJ/t (clinker) and the heat loss caused by the temperature swing between MEA scrubbing and DRM (**Figure S13, TableS8 and S9**) makes the constructed thermal decomposition system utra-high energy consumptions. The significant achievement of a 37.5% reduction of overall energy consumption in the CaDRM system come from not only the lower operating temperature, but also avoiding the unreasonable temperature swing between cooling down the flue gas for the CO_2 capture by MEA-scrubbing and raising up again for the CO_2 conversion by DRM reaction.

Accordingly, the economic evaluation based on the 2500 t/d (clinker) production shows that the operating cost of the CaDRM system is $340.26k/d, composed of the raw meal ($35.10k), nature gas feed ($200.43k), catalysts attrition ($46.80k), electricity for ASU and PSA unit ($37.64k) (**Table 1**). Among them, the price of nature gas (NG) is the cost-dominant factor for the operating cost of CaDRM process (**Figure S14**). On the other hand, with the incomes of $1017.75k/d returned from the 2500 t/d clinker and 1956 t/d syngas products, the revenue of CaDRM process will be about $407.10/t (clinker), perfectly able to offset the operating cost of $136.10/t (clinker), and achieve a net profit of $271.0/t (clinker) (**Table 1**). More importantly, the product of syngas with the molar ratio of H_2 to CO of 1 can be further utilized downstream for higher value-added chemicals and fuels[43,44]. On the contrary, although the operating cost of the pristine $CaCO_3$ thermal decomposition is as low as $81.24/t (clinker), the operating costs of CCU of the MEA scrubbing and the DRM to produce syngas were calculated as high as $65.0/t ($CO_2$)] and $143.78/t ($CO_2$), respectively (**Figure 5e**). Based on the average CO_2 emission of 0.745 t/t (clinker), the overall operating cost of the $CaCO_3$ thermal decomposition with CCUS route is calculated to be at least $290.02/t (clinker), which is 113.09% higher than the proposed CaDRM route for clinker and syngas productions, letting alone the additional operating costs of CO_2 compression and transportation for the separated CCU processes in general.

Conclusion

In this study, a novel pathway of "Carbonate Dry Reforming of Methane (CaDRM)" strategy was proposed and successfully through converting the raw meal ($CaCO_3$) directly into the cement clinker precursor (CaO) and syngas by CH_4. Thanks to the cement compatible catalyst of Ni/CaO, the CaDRM

reaction achieves a complete conversion of $CaCO_3$ at a 90% conversion efficiency of CH_4 at relatively lower temperature of 700ºC. More significantly, the feasibility of CaDRM was further demonstrated by adopting the cement raw meal, with the excellent conversion efficiency of 95% for the main component of $CaCO_3$, 90% for CH_4, and selectivity of 91% for syngas, respectively. Based on the process simulations, the proposed CaDRM system enabled a 37.2% reduction of the CO_2 emissions and a 37.5% reduction in overall energy consumption in comparison with the conventional $CaCO_3$ thermal decomposition system with CCU. Economic analysis reveals that the operating costs of this novel CaDRM stands at \$136.10/t (clinker), 113.09% lower than that of the conventional clinker manufacturing integrated with CCU processes of MEA-scrubbing and DRM-conversion. Notably, CaDRM process for co-production clinker and syngas can achieve revenue of \$407.10/t (clinker), with a net profit of \$271.0/t (clinker). Accordingly, this newly proposed CaDRM technology will reduce CO_2 emissions and improve the economics at the same time.

Acknowledgements

We acknowledge the financial support from the National Natural Science Foundation of China (22278126, 22250005), Intergovernmental International Science and Technology Innovation Cooperation Key Project (2021YFE0112800) and the Fundamental Research Funds for the Central Universities (2022ZFJH04). The UK author would like to thank the financial support of the EU RISE project OPTIMAL (Grant Agreement No: 101007963).

Data Availability

The data that support the findings of this study are available within the article and supplementary information or from the corresponding authors on reasonable request. Source data are provided with this paper.

Competing interests

The authors declare no competing interests.

References

1. Tian, S., Jiang, J., Zhang, Z. & Manovic, V. Inherent potential of steelmaking to contribute to decarbonisation targets via industrial carbon capture and storage. Nat. Commun. **9**, 4422 -4429 (2018).
2. Wu, T., Ng, S.T. & Chen, J. Deciphering the CO_2 emissions and emission intensity of cement sector in China through decomposition analysis. J. Clean. Prod. **352**, 131627-131641 (2022).
3. Yang, Y., et al. Mapping global carbon footprint in China. Nat. Commun. **11**, 2237-2244 (2020).
4. Fennell, P.S., Davis, S.J. & Mohammed, A. Decarbonizing cement production. Joule **5,** 1305-1311 (2021).
5. Mowbray, B.A.W., Zhang, Z.B., Parkyn, C.T.E. & Berlinguette, C.P. Electrochemical cement clinker precursor production at low voltages. ACS Energy Lett. **8**, 1772-1778 (2023).
6. Santos, T.A., Cilla, M.S. & Ribeiro, e.D.V. Use of asbestos cement tile waste (ACW) as mineralizer in the production of Portland cement with low CO_2 emission and lower energy consumption. J. Clean. Prod. **335**, 130061-130072 (2022).
7. Shah, I.H., Miller, S.A., Jiang, D. & Myers, R.J. Cement substitution with secondary materials can reduce annual global CO_2 emissions by up to 1.3 gigatons. Nat. Commun. 13, 5758 (2022).
8. Watari, T., Cao, Z., Hata, S. & Nansai, K. Efficient use of cement and concrete to reduce reliance on supply-side technologies for net-zero emissions. Nat. Commun. 13, 4158 (2022).
9. Wojtacha-Rychter, K., Kucharski, P. & Smolinski, A. Conventional and alternative sources of thermal energy in the production of cement—An impact on CO_2 emission. Energies **14**, 1539 (2021).

10. Rumayor, M., Fernández-González, J., Domínguez-Ramos, A. & Irabien, A. Deep decarbonization of the cement sector: A prospective environmental assessment of CO_2 recycling to methanol. ACS Sustain. Chem. Eng. 10, 267-278 (2022).
11. Benhelal, E., Shamsaei, E. & Rashid, M.I. Novel modifications in a conventional clinker making process for sustainable cement production. J. Clean. Prod. **221**, 389-397 (2019).
12. Erans, M., et al. Pilot testing of enhanced sorbents for calcium looping with cement production. Appl. Energy **225**, 392-401 (2018).
13. Sun, J., et al. MOF-Derived Ru_1Zr_1/Co dual-atomic-site catalyst with promoted performance for Fischer–Tropsch synthesis. J. Am. Chem. Soc. **145,** 7113-7122 (2023).
14. Centi, G. & Perathoner, S. The chemical engineering aspects of CO_2 capture, combined with its utilisation. Curr. Opin. Chem. Eng. **39**, 100879 (2023).
15. Otto, A., Grube, T., Schiebahn, S. & Stolten, D. Closing the loop: captured CO_2 as a feedstock in the chemical industry. Energy Environ.Sci. **8,** 3283-3297 (2015).
16. Yang, C., et al. Intrinsic mechanism for carbon dioxide methanation over Ru-based nanocatalysts. ACS Catal. **13**, 11556-11565 (2023).
17. Zhang, Z., et al. Cement clinker precursor production in an electrolyser. Energy Environ. Sci. **15**,5129-5136 (2022).
18. Zhang, C.-Y., Yu, B., Chen, J.-M. & Wei, Y.-M. Green transition pathways for cement industry in China. Resour. Conserv. Recy. **166**, 105355 (2021).
19. Chen, X., Matar, M.G., Beatty, D.N. & Srubar, W.V., III. Retardation of Portland cement hydration with photosynthetic algal biomass. ACS Sustain. Chem. Eng. **9**, 13726-13734 (2021).
20. Benhelal, E., Shamsaei, E. & Rashid, M.I. Challenges against CO_2 abatement strategies in cement industry: A review. J. Environ. Sci. **104**, 84-101 (2021).
21. Zhu, Q., et al. Enhanced CO_2 utilization in dry reforming of methane achieved through nickel-mediated hydrogen spillover in zeolite crystals. Nat. Catal. **5**, 1030-1037 (2022).
22. Chen, L., et al. Ternary NiMo-Bi liquid alloy catalyst for efficient hydrogen production from methane pyrolysis. Science **381**, 857-861 (2023).
23. Giardini A., Salotti C. & Lakner J. Synthesis of graphite and hydrocarbons by reaction between calcite and hydrogen. Science **159**, 317-319(1968).
24. Reller, A., Padeste, C. & Hug, P. Formation of organic carbon compounds from metal carbonates. Nature **329**, 527-529 (1987).
25. Baldauf-Sommerbauer, G., Lux, S. & Siebenhofer, M. Sustainable iron production from mineral iron carbonate and hydrogen. Green Chem. **18**, 6255-6265 (2016).

26. Sun, S., et al. Integrated CO_2 capture and utilization with CaO-alone for high purity syngas production. Carbon Capture Sci. Technol. **1**, 100001 (2021).
27. Xue, Z., et al. Co-thermal in-situ reduction of inorganic carbonates to reduce carbon-dioxide emission. Sci. China Chem. **66**, 1201-1210 (2023).
28. Shi, S., et al. Hydrogenation of calcium carbonate to carbon monoxide and methane. Fuel **354**, 129385 (2023).
29. Zhu, Q., et al. Enhanced CO_2 utilization in dry reforming of methane achieved through nickel-mediated hydrogen spillover in zeolite crystals. Nat. Catal. **5**, 1030-1037 (2022).
30. Zhang, Q., Akri, M., Yang, Y. & Qiao, B. Atomically dispersed metals as potential coke-resistant catalysts for dry reforming of methane. Cell Rep. Phys. Sci. **4**, 101291-101304 (2023).
31. Wang, J., et al. Investigation of atom-level reaction kinetics of carbon-resistant bimetallic NiCo-reforming catalysts: Combining microkinetic modeling and density functional theory. ACS Catal. **12,** 4382-4393 (2022).
32. Galdeano, C., Cook, M. A. & Webber, M. E. Multilayer geospatial analysis of water availability for shale resources development in Mexico. Environ. Res. Lett. **12**, 084014 (2017).
33. Yu, Y. Mechanisms for the accumulation of deep gas in the southern Songliao Basin. China. J. Pet. Sci. Eng. **182**, 106302 (2019).
34. Shao, B., et al. Synergistic promotions between CO_2 capture and in-situ conversion on Ni-CaO composite catalyst. Nat. Commun. 14, 996 (2023).
35. Steinfeld, A. Solar combined thermochemical processes for CO_2 mitigation in the iron, cement, and syngas industries. Energy 19, 1077-1081 (1994).
36. Upham, D.C., et al. Catalytic molten metals for the direct conversion of methane to hydrogen and separable carbon. Science **358**, 917-921 (2017).
37. Tian, S., Yan, F., Zhang, Z. & Jiang, J. Calcium-looping reforming of methane realizes in situ CO_2 utilization with improved energy efficiency. Sci. Adv**. 5**, eaav5077 (2019).
38. Kim, S.M., et al. Integrated CO_2 capture and conversion as an efficient process for fuels from greenhouse gases. ACS Catal. **8**, 2815-2823 (2018).
39. Liu, H.-X., et al. Partially sintered copper–ceria as excellent catalyst for the high-temperature reverse water gas shift reaction. Nat. Commun. **13**, 867 (2022).
40. Rezaei, E. & Dzuryk, S. Techno-economic comparison of reverse water gas shift reaction to steam and dry methane reforming reactions for syngas production. Chem. Eng. Res. Des. **144**, 354-369 (2019).
41. Monteiro, J. & Roussanaly, S. CCUS scenarios for the cement industry: Is CO_2 utilization feasible?

J. CO_2 Utiliz. **61**, 102015 (2022).

42. Nhuchhen, D.R., Sit, S.P. & Layzell, D.B. Alternative fuels co-fired with natural gas in the pre-calciner of a cement plant: Energy and material flows. Fuel **295**, 120544(2021).

43. Pan, X., Jiao, F., Miao, D. & Bao, X. Oxide–zeolite-based composite catalyst concept that enables syngas chemistry beyond Fischer–Tropsch synthesis. Chem. Rev. **121**, 6588-6609 (2021).

44. Wang, C., et al. Direct conversion of syngas to ethanol within zeolite crystals. Chem. **6**, 646-657 (2020).